In-Process Ultrasonic Measurements of Orientation and Disorientation Relaxation of High-Density Polyethylene/ Polyamide-6 Composites with Compatibilizer

Congmei Lin, Huimin Sun, Shan Wang, Jian Huang, Jiang Li, Shaoyun Guo

The State Key Laboratory of Polymer Materials Engineering, Polymer Research Institute of Sichuan University, Chengdu 610065, China

Received 31 July 2009; accepted 28 September 2009
DOI 10.1002/app.31566
Published online 1 December 2009 in Wiley InterScience (www.interscience.wiley.com).

ABSTRACT: The relaxation processes of orientation and disorientation of melts of high-density polyethylene (HDPE) and polyamide-6 (PA6) blends compatibilized with a compatibilizer precursor (CP) of HDPE-grafted maleic anhydride (HDPE-*g*-MAH) were investigated in a restricted channel using real-time ultrasonic technique. The experimental results showed that the evolution of ultrasonic velocity of HDPE/PA6 blends during the orientation or disorientation processes could be described by the exponential equation from which the maximum orientation degree and relaxation time could be obtained. Subsequently, the effects of CP on the relaxation processes of orientation and disorientation were studied. In addition, the relations of the CP content and the morphology and viscosity were investigated by scanning electron microscope analysis and rheological tests. © 2009 Wiley Periodicals, Inc. J Appl Polym Sci 116: 320–327, 2010

Key words: high-density polyethylene; polyamide-6; compatibilizer; morphology; in-process; ultrasound

INTRODUCTION

In the last decades, polymer blending in the internal mixer, double-roll open mill, and single- and twin-screw extruder has been proved to be an economical, rapid, and versatile way to obtain desirable properties in the industrial field.[1–5]

As one of the most commonly used general plastics, polyethylene (PE) has the advantages of low cost, light weight, nontoxicity, good chemical stability, and low moisture absorbance,[6] and it is extensively applied to produce film, container, pipe, electric wire and cable, monofilament, and so on. On the other hand, polyamide (PA) is an engineering thermoplastic with high strength, wear resistance, and heat stability, and it is widely applied in automobile, electrical equipments, mechanical parts, as well as textile.[7] The blending of PE and PA provides an effective way to make full use of their respective advantages and has been widely investigated in the academic and industrial fields.[8–11]

Because of the differences in molecular polarity and chain structure, PE/PA blends are thermodynamically immiscible, resulting in inferior performance of final products. A common and convenient method to improve the properties of PE/PA blends is the addition of a compatibilizer precursor (CP).[6,12–20] It is recognized that the common mechanism is that a grafting reaction takes place between the epoxide or acidic functional groups of CP and the carboxyl/amine terminal groups of PA at PE–PA interface to *in situ* form a PE-*g*-PA copolymer, which generates a covalent bond between PE and PA.[6,12,15] As a result, the interfacial adhesion between the matrix and the dispersed phase is enhanced. Therefore, the addition of CP could result in a significant change in the morphology and properties of PE/PA composites, including the mechanical properties,[6] rheological behaviors,[12] thermal stability,[6] melting and crystallization behaviors.[16,17,21]

However, the real-time studies on the development of molecular structure of PE/PA6 blends during the melt processing have been limited. The products of PE/PA composites are usually obtained from extrusion and injection molding. During these processes, molecular chains align along a specific direction when subjected to a shear stress. The orientation is of great interest in the academic and industrial fields because of its significant influences on the physical properties of final products. In polyolefin/PA blends, it is found that the orientation contributes to the improvement of mechanical properties[22]

Correspondence to: J. Li (li_jiang@scu.edu.cn) or S. Y. Guo (nic7702@scu.edu.cn).

Contract grant sponsor: National Natural Science Foundation of China; contract grant number: 50973075.

Contract grant sponsor: Scientific Research Foundation for the Returned Overseas Chinese Scholars, State Education Ministry; contract grant number: 2008890-19-8.

and barrier properties.[23] The orientation is a complicated process, which is affected by many factors, for instance, component ratio, temperature, viscosity ratio, and shear stress. In addition, interfacial interaction between two components is believed to be related to the orientation in the compatibilized systems. However, researches on the effects of CP on the orientation of polymer chains are relatively limited, especially in the molten state during processing because of the difficulty in the introduction of in-process characterization methods.

It is well known that in-process diagnostics and control play a key role in improving the final product performance during polymer processing.[24–26] As a kind of in-process measurement, ultrasound has gained increasing attention in the field of polymer diagnosis because of its nondestructiveness, noninvasiveness, cost-effectiveness, convenient installation, quick feedback, and high sensitivity to material properties. Ultrasonic measurements have been proved to be an effective means to characterize polymer structure, properties, and processing conditions.[27,28]

In our previous work,[29] the ultrasonic velocity has been used to investigate the relaxation of orientation and disorientation of low-density polyethylene and polypropylene melts. The results indicate that the ultrasonic velocity is sensitive to the relaxation behaviors of orientation and disorientation of polymer melts and can characterize the degree of orientation. The change of ultrasonic velocity with time is found to obey an exponential law from which the relaxation time of orientation and disorientation can be obtained. Consequently, the ultrasonic measurements can be used to detect the anisotropic behaviors in polymer melts.

However, the fundamental understanding of the effects of interaction between the components in polymer blends on the relaxation of orientation and disorientation is still unclear. In this work, we focus on the blends of high-density polyethylene (HDPE) and polyamide-6 (PA6) with a HDPE-grafted maleic anhydride (HDPE-*g*-MAH) as a CP prepared with a twin-screw extruder. The main objective of this study is to investigate the processes of chain orientation and disorientation of HDPE/PA6 blends by in-process ultrasonic measurements. The studies on the effects of CP content on the morphology and rheological behaviors are also conducted.

EXPERIMENTAL

Materials

A HDPE (5000S) with a melt flow index of 0.93 g/10 min (190°C, 2.16 kg) and a density of 0.954 g/cm^3, provided by Lan Zhou Petroleum Chemical, China, was used. As a dispersed phase, a PA6 (M3400) with an intrinsic viscosity of 3.4 dL/g and a density of 1.14 g/cm^3 was supplied by Guangdong Xinhui Meida Nylon, China. A HDPE-*g*-MAH (GPM119) with a grafting degree of 0.8 wt % was used as a CP, obtained from Ningbo Nengzhiguang New Materials Technology, China.

Blend preparation

Before melt blending, PA6 was carefully dried in a vacuum oven at 95°C for 12 h to reduce the influence of moisture content and avoid the hydrolytic degradation of PA6 during processing; HDPE and HDPE-*g*-MAH were dried in an oven at 80°C for 12 h. Blends of HDPE and PA6 at composition ratio of 80/20 by weight with CP of 0, 2, 5, 10, 20 phr were labeled PA20, PA20-2, PA20-5, PA20-10, and PA20-20, respectively. The blends were prepared with a twin-screw extruder at a set screw speed of 15 Hz and a die set temperature of 235°C.

Scanning electron microscope

Morphological characterization was carried out with a scanning electron microscope (SEM, XL30FEG, Philips). The samples were prepared by compression molding after twin-screw extrusion and then fractured cryogenically in liquid nitrogen. The fractured surfaces were coated with a thin layer of gold in a vacuum chamber for conductivity after etching by formic acid for 8 h. The number-average diameter (d_n) and volume-average diameter (d_v) of the dispersed particles could be determined by:

$$d_n = \sum (n_i d_i) / \sum n_i \quad (1)$$

$$d_v = \left\{ \sum (n_i d_i^3) / \sum n_i \right\}^{1/3}, \quad (2)$$

where d_i is the diameter of the particles and n_i is the number of particles.

Rheological measurements

Dynamic rheological measurements of the blends were performed on an oscillatory rheometer (AR1500EX, TA) under a nitrogen atmosphere at 230°C. The measurements were conducted with 25-mm parallel plate geometry and a 1.0-mm sample gap. The viscoelastic properties were measured in the frequency range of 0.01–100 Hz. The strain was determined to be 5% to keep within the linear viscoelastic region.

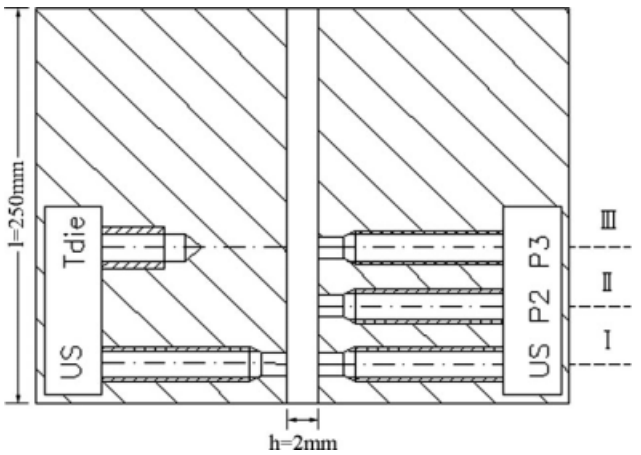

Figure 1 Schematic representation of the ultrasonic monitoring system used in the experiment.

Ultrasonic measurements

The relaxation behaviors of orientation and disorientation were characterized by in-process ultrasonic measurements. The in-process ultrasonic inspection system comprised of two main components: a capillary rheometer (RH7, Malvern) and an instrumented slit die, which was fitted to the barrel exit of the capillary rheometer. The capillary rheometer was used to preheat samples and give rise to a certain shear stress through the movement of the piston. In this work, the shear rate ($\dot{\gamma}$) could be calculated from $\dot{\gamma} = 6v\pi R^2/h^2w$, where v, R, h, and w are the velocity of the piston, barrel radius of capillary rheometer, slit height, and slit width, respectively. The slit die was equipped with two ultrasonic sensors (US) in cross-section I, a pressure transducer (P2) in cross-section II, a pressure transducer (P3) and a die temperature sensor (T_{die}) in cross-section III, as illustrated in Figure 1. The cross-sections I, II, and III were equidistantly located from the exit of the slit die. In the slit die, the flow channel had a width of 20 mm, a height of 2 mm, and a length of 250 mm. The ultrasonic sensors and pressure transducers were flush-mounted in order not to disturb the flow of the melts. The slit die was heated by a wrapped-on heating jacket with a piecewise proportion integral differential controller. The transmission technique was adopted in this experiment with two ultrasonic sensors installed in the opposite side of the slit die. An ultrasonic sensor generated acoustic pulse, and then the acoustic pulse traveled through polymer melt and received by another ultrasonic sensor. In this experiment, the ultrasonic velocity (C) was calculated from the time delay difference (Δt) between two consecutive echoes and the height of slit die ($h = 2$ mm):

$$C = 2h/\Delta t. \tag{3}$$

RESULTS AND DISCUSSION

Effects of CP on the morphology

The influences of CP content on the morphology and the size distribution of HDPE/PA6 composites are shown in Figure 2. The noncompatibilized blend

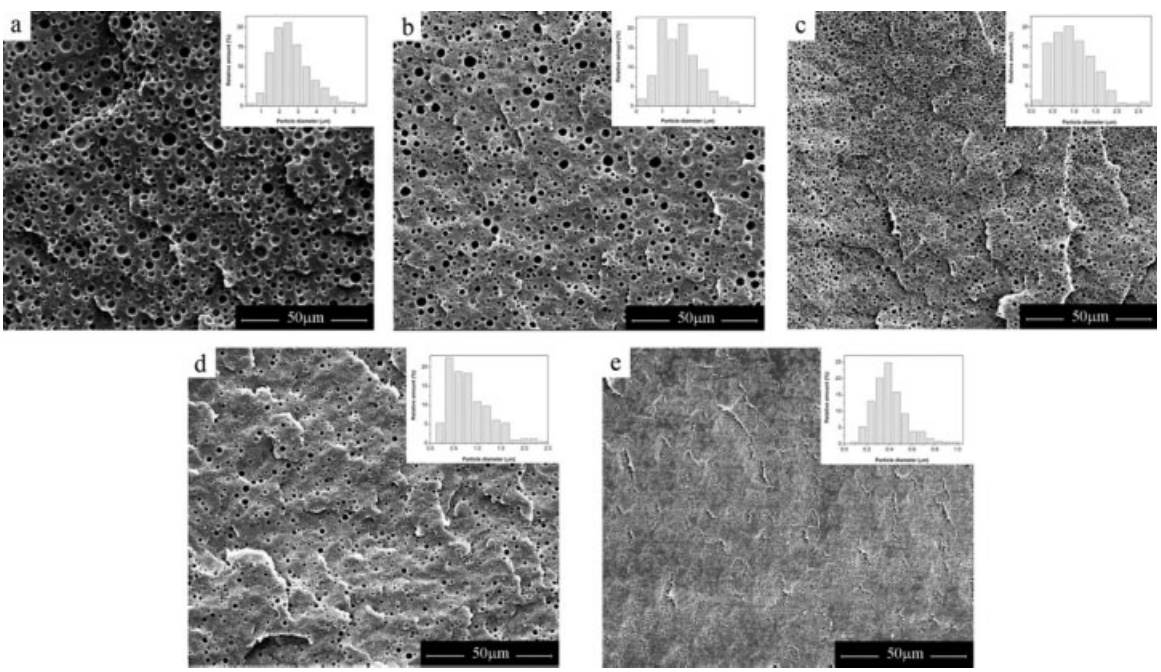

Figure 2 SEM micrographs and particle size distribution of HDPE/PA6 blends with 20 wt % PA6: (a) without CP, (b) with 2 phr CP, (c) with 5 phr CP, (d) with 10 phr CP, and (e) with 20 phr CP.

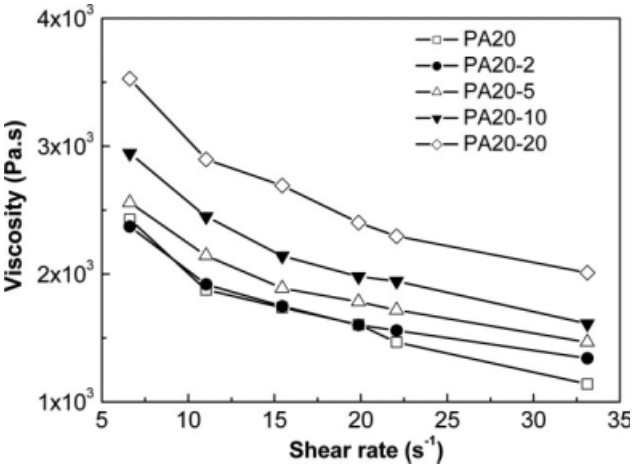

Figure 3 Relationship between viscosity and shear rate of HDPE/PA6 blends with different CP contents.

[Fig. 2(a)] shows a typical morphology for thermodynamically immiscible system with the phase separation. PA6 is dispersed in HDPE matrix in the form of spherical particles, known as the sea island structure. The particles vary greatly in size from 0.2 to 6.5 μm with $d_n = 2.61$ μm, revealing high polydispersity. Figure 2(b–e) exhibits the morphology and particle size distribution of the compatibilized blends with different CP content. The d_n of the dispersed particles decreases from 2.61 to 0.40 μm with increasing CP content. The d_v of the dispersed particles shows the same tendency. The results can be ascribed to the decreased interfacial tension between two components and the inhibited coalescence of droplets to form larger domains. The results display that HDPE-*g*-MAH is an effective compatibilizer for HDPE/PA6 composites because of more homogeneous dispersion and ameliorated interfacial adhesion in the compatibilized blends. The evolution of morphology is consistent with the findings reported earlier.[30]

Effects of CP on the rheological properties

The melt viscosities of HDPE/PA6 composites are investigated to evaluate the effects of CP content on the processing properties. The viscosity in molten state during extrusion can be measured by the pressure transducers in the slit die:

$$\eta = \Delta P h^3 w / 12 L Q, \tag{4}$$

where ΔP is the pressure drop, L describes the center-to-center distance between pressure transducers P2 and P3, and Q represents the volume flow rate. As expected, the viscosities of the compatibilized blends are higher than that of the noncompatibilized one. As can be seen in Figure 3, the viscosities of HDPE/PA6 blends depend significantly on CP content. With regard to HDPE/PA6 binary blend without CP, the lowest viscosity is observed. When the CP content is 2 phr, a slight increase is observed in the viscosity at higher shear rate, compared with the counterpart without CP. The viscosity increases obviously with increasing CP content over the whole shear rate range. The underlying mechanism accounting for these behaviors is that a grafting reaction takes place between the acid anhydride groups of HDPE-*g*-MAH and the amine end-groups of PA6 at the blend interface, *in situ* formed a HDPE-*g*-PA6 copolymer whose main chains and branched chains have the same compositions as the matrix and dispersed phase, respectively, leading to partially cross-linked structure.[12,16] Consequently, the compatibility of HDPE and PA6 is improved, and the interfacial adhesion strength between the matrix and dispersed phase is enhanced.

The melt viscosities can also be obtained by means of dynamic rheological measurements. Figure 4 illustrates the effects of CP on the complex viscosities. The results are in close agreement with the findings obtained by the pressure transducers during extrusion. It is clear that with the addition of CP, the complex viscosities of the blends increase. The change of viscosities is consistent with the data of Ohlsson et al.[31]

Effects of CP on the relaxation behaviors of orientation and disorientation

The velocity of longitudinal waves (C) is a function of the bulk modulus (K) and the density (ρ), according to the following equation:

$$C = \sqrt{\frac{K}{\rho}}. \tag{5}$$

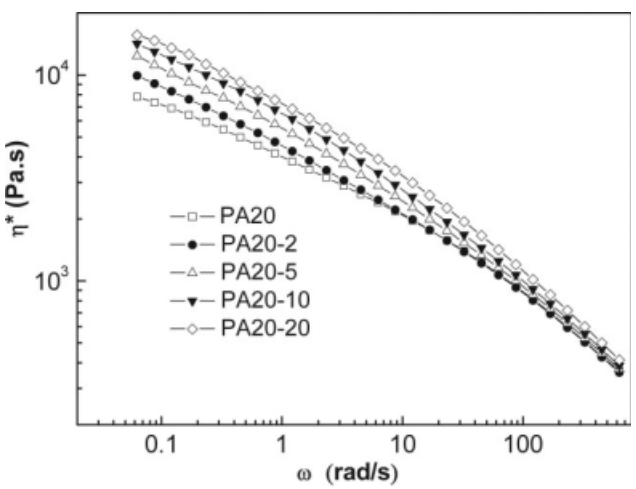

Figure 4 The complex viscosity as a function of frequency for HDPE/PA6 blends with different CP contents.

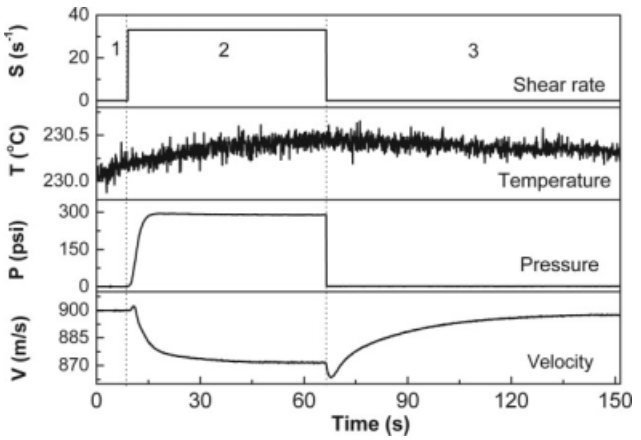

Figure 5 The typical variation of the shear rate, melt temperature, pressure, and ultrasonic velocity with time for HDPE/PA6 blends with 10 phr CP.

During the extrusion, the density of polymer melts is regarded as a constant value, and therefore, the velocity of ultrasound is only dependent on the bulk modulus, which varies with the change of melt pressure, temperature or molecular orientation.

As an example, Figure 5 presents the typical variation of the shear rate, temperature, pressure, and ultrasonic velocity with the processing time for HDPE/PA6 (80/20 wt %) blends with 10 phr CP. During the whole test, the temperature is almost kept constant; accordingly, the influence of temperature on the ultrasonic velocity can be neglected. As can be seen in Figure 5, in terms of shear rate, the process could be divided into three stages: the static stage (0–9 s), the shear stage (9–66 s), and the postshear stage (66–156 s). In the static stage, the shear rate and pressure are zero, so there is no orientation. In the shear stage, polymer melts are pushed through the slit die with the piston of the capillary rheometer moving at a constant rate. The shear rate is invariable with a value of 33.1 s^{-1}. The pressure increases sharply and then maintains constant. Because of the shear stress, the molecular chains are oriented along the flow direction. However, the orientation is a relaxation process due to the friction between molecular chains and the response to outer action is slower than the pressure. And in the postshear stage, the piston stops and the shear rate goes back to zero. The pressure decreases suddenly to zero. The disorientation occurs because of the disappearance of the shear stress. Likewise, the disorientation is also a relaxation process.

In the latter two stages, the ultrasonic velocity is affected by the pressure and orientation simultaneously, which are mutual competitive processes. An enhancement in the melt pressure leads to an increase of K, whereas an increase in the degree of orientation results to a decrease of K in the direction perpendicular to the shear flow. At the beginning of the latter two stages, the change of ultrasonic velocity is predominated by the pressure owing to its abrupt variation. But then the ultrasonic velocity varies in the opposite direction induced by the orientation or the disorientation. At the end of these two stages, the ultrasonic velocity levels off, suggesting the orientation or disorientation is completed.

In this work, the shear and postshear stages are applied to investigate the orientation and disorientation, respectively. To cancel out the influences of the temperature and pressure, the ultrasonic velocity is corrected according to the Ref. [32]. The ultrasonic velocity mentioned later has been corrected.

To quantitatively determine the influences of CP content on orientation and disorientation, Figure 6 shows two models, which are established to describe

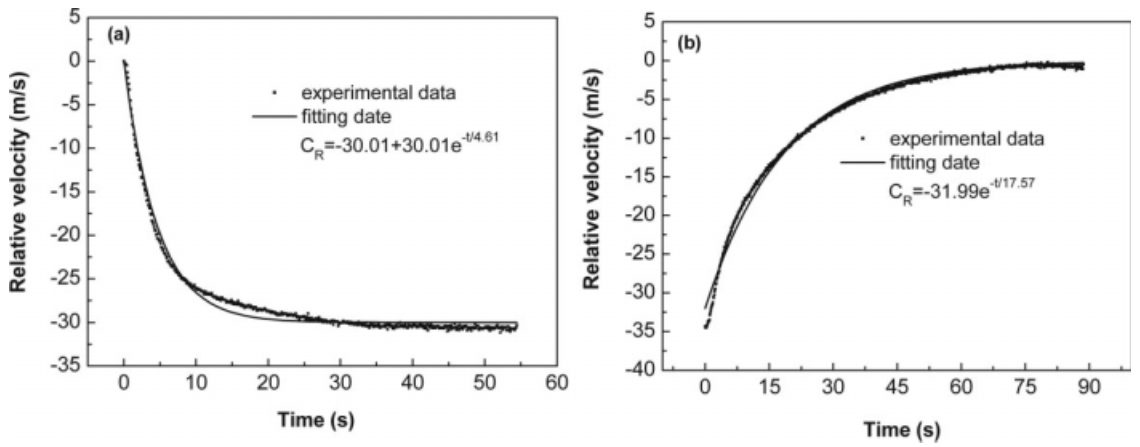

Figure 6 Modeling of the relaxation processes for HDPE/PA6 blends with 10 phr CP: (a) orientation and (b) disorientation.

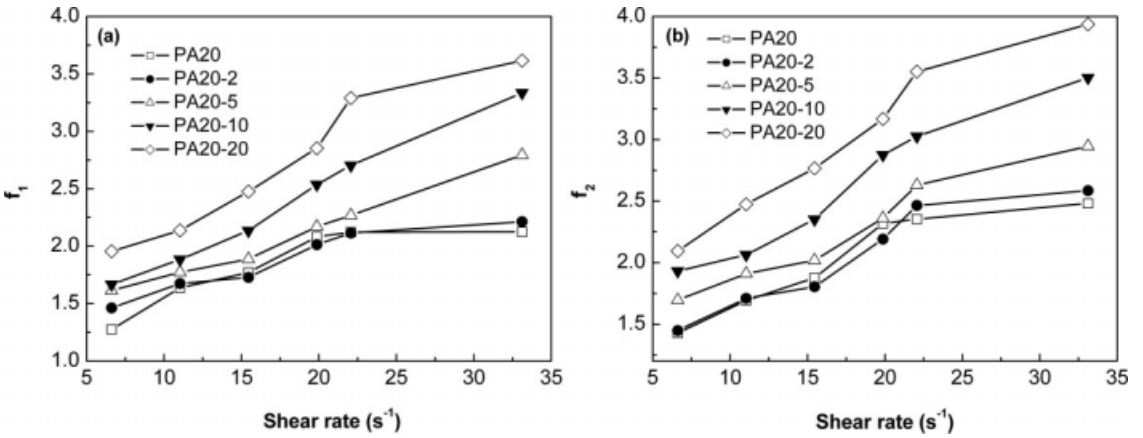

Figure 7 The maximal degree of orientation as a function of shear rate for HDPE/PA6 blends: (a) f_1 and (b) f_2.

the relaxation processes of orientation and disorientation in Figure 5.

$$C_{R1}(t) = C_1\left(1 - e^{-t/\tau_1}\right) \tag{6}$$

$$C_{R2}(t) = C_2 e^{-t/\tau_2}, \tag{7}$$

where the subscripts 1 and 2 represent the processes of orientation and disorientation, respectively, C is the maximum relative velocity, τ is the relaxation time, C_R is the relative ultrasonic velocity with the velocity $C(t)$ at time t subtracting the value in the unoriented state ($C(t_0)$):

$$C_R(t) = C(t) - C(t_0). \tag{8}$$

It can be seen from Figure 6 that the exponential eqs. (6) and (7) could well describe the experimental data of HDPE/PA composite. In the molten state, the orientation of HDPE/PA6 composite melts includes the orientation of the HDPE matrix and dispersed PA6 phase. It should be emphasized that the orientation and disorientation are related to the whole blends, and it is unable to differentiate the respective orientation and disorientation of HDPE and PA6 phases.

As illustrated in Figure 6, C_1 and C_2 are 30.01 and 31.99 m/s, respectively. These two values are approximately equal, indicating that the oriented chains are almost totally disoriented during the post-shear stage. However, it can be seen that τ_1 (4.61 s) is much less than τ_2 (17.57 s). This result can be attributed to the different mechanisms of orientation and disorientation. Although the disorientation is a reverse process of orientation, the latter is not spontaneous. The existence of external force is thermodynamically in favor of the motion of molecular chains, therefore, leads to a quicker relaxation of orientation than that of disorientation.

In addition, we use f_1 and f_2 to represent the maximum degree of orientation during orientation and disorientation, respectively:

$$f_1\% = |C_1/C(t_0) \times 100\%| \tag{9}$$

$$f_2\% = |C_2/C(t_0) \times 100\%|. \tag{10}$$

The higher the values of f_1 and f_2, the bigger the maximum degree of orientation. Figure 7 describes that the values of f_1 and f_2 increase with CP content at the invariable shear rate. In our previous work,[32] the maximum degree of orientation of HDPE is affected by its melt viscosity, and the higher the melt viscosity, the higher the maximum degree of orientation. This law is still valid for HDPE/PA6 blends. As stated earlier, the addition of CP leads to an increase in the melt viscosity; as a consequence, the maximum degree of orientation of HDPE/PA6 blends increases with the increase of CP content. In addition, Figure 7 shows that the maximum degree of orientation of HDPE/PA6 blends with or without CP increases with increasing shear rate. This may be a result of the higher stress that can result in more deformation of molecular chain.

The dependence of the relaxation time of orientation (τ_1) on CP content in Figure 8 shows that τ_1 increases with increasing CP content. The improvement of interfacial adhesion is believed to be the major contribution to this behavior. As mentioned previously, a HDPE-*g*-PA copolymer formed at the interface between HDPE matrix and dispersed PA6 phase with the addition of CP can raise the interfacial friction under shear stress, and therefore, cause the slowdown of molecular chain motion. It also can be seen from Figure 8 that τ_1 is sensitive to shear rate. The decrease of τ_1 with shear rate shows that the stress can markedly affect the speed of orientation. It is in accordance with the fact that the

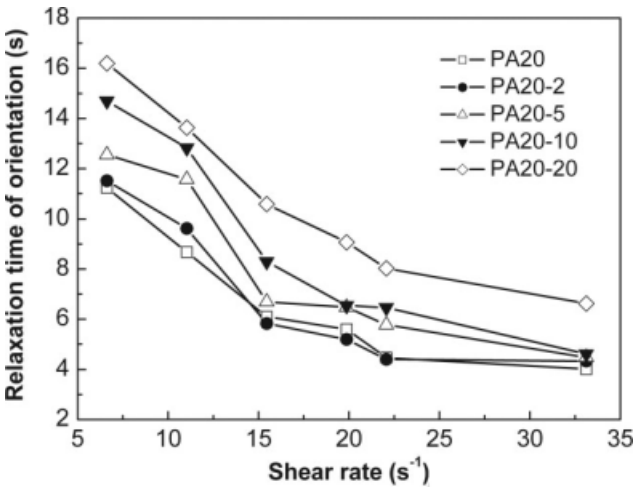

Figure 8 The relaxation time of orientation versus shear rate for HDPE/PA blends compatibilized with different amounts of CP.

orientation status is a thermodynamically nonequilibrium state and relies on the stress.

As revealed in Figure 9, an increase in the relaxation time of disorientation (τ_2) is also observed with increasing CP content. The disorientation takes place after the cession of shear, with its relaxation time related to the molecular structure parameters of HDPE/PA6 composites such as composite ratio, molecular weight of each component, and intermolecular interaction between two components. In this case, the evolution of τ_2 is determined by the intermolecular interaction between HDPE matrix and dispersed PA6 phase. The addition of CP results in a grafting reaction to form a copolymer of HDPE-*g*-PA, which trends to concentrate at the interface, and therefore, the interfacial interaction is enhanced and the compatibility is improved. It is worth noting that

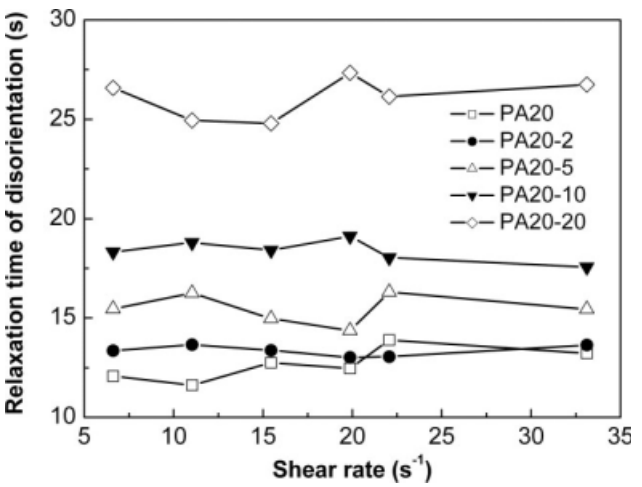

Figure 9 The relaxation time of disorientation versus shear rate for HDPE/PA blends compatibilized with different amounts of CP.

TABLE I
The Characteristic Relaxation Time Defined by ω_c and Average Relaxation Time of Disorientation Detected by Ultrasonic Measurements

Blends	$1/\omega_c$ (s)	Average relaxation time of disorientation (s)
PA20	2.47×10^{-2}	12.66
PA20-2	2.49×10^{-2}	13.35
PA20-5	3.65×10^{-2}	15.47
PA20-10	4.74×10^{-2}	18.38
PA20-20	7.56×10^{-2}	26.09

τ_2 is independent on shear rate in the examined shear rate range. Compared with orientation, the process of disorientation is spontaneous; as a consequence, it is unrelated to the external conditions during processing. This experimental result suggests to some extent that τ_2 could be served as a kind of characteristic relaxation time of polymer melts.

The relaxation behaviors of polymer melts are also analyzed by the dynamic rheological measurements. According to Wang et al.,[33] the reciprocal of crossover frequency (ω_c) of the storage modulus (G') and loss modulus (G'') is considered as a single characteristic relaxation time. The characteristic relaxation times of HDPE/PA6 blends with or without CP are presented in Table I. The characteristic relaxation time is found to increase as the CP content increases, which is in agreement with the variation of the average relaxation time of disorientation. It is noteworthy that the average relaxation time of disorientation acquired from ultrasonic measurements is two to three order of magnitude higher than the characteristic relaxation time obtained from dynamic rheological measurements. It has been correlated with the differences between two methods: the ultrasonic measurements are carried out at large deformation, concerning with the whole molecular chain, but the rheological measurements are conducted at small deformation.

CONCLUSIONS

HDPE-*g*-MAH was used as a CP in the blends of HDPE and PA6 to examine the influences of CP on the properties of blends. The experimental results demonstrated that:

1. The HDPE/PA6 binary composition presented two-phase morphology because of the thermodynamic immiscibility of the components. It was found that the addition of CP could evidently diminish the particle size (d_n and d_v) of dispersed phase and ameliorate the homogeneous dispersion due to a decrease in the

interfacial tension and an enhancement in the interfacial adhesion.
2. The compatibilized blends displayed a very pronounced increase in the viscosities, compared with the uncompatibilized one.
3. In-process ultrasonic measurements with the advantages of nondestructiveness, cost-effectiveness, and high sensitivity to material properties and process conditions were utilized to research the relaxation processes of orientation and disorientation. The experimental results indicated that the maximal degree of orientation of the blends depended on the CP content, owing to the improved viscosity. An increase in the relaxation time of orientation and disorientation with CP content was also observed.

In summary, the change in the morphology, rheological behaviors, and the relaxation processes of orientation and disorientation of HDPE/PA6 blends with different CP concentration could be attributed to the chemical reaction occurred between the acid anhydride groups of HDPE-*g*-MAH and the amine end-groups of PA6, *in situ* formed a HDPE-*g*-PA copolymer, which enhanced the interfacial interaction of HDPE matrix and dispersed PA6 phase.

References

1. Yang, Z.; Han, C. D. Macromolecules 2008, 41, 2104.
2. Miwa, Y.; Usami, K.; Yamamoto, K.; Sakaguchi, M.; Sakai, M.; Shimada, S. Macromolecules 2005, 38, 2355.
3. Hsu, J. Y.; Hsieh, I. F.; Nandan, B.; Chiu, F. C.; Chen, J. H.; Jeng, U. S.; Chen, H. L. Macromolecules 2007, 40, 5014.
4. Tomova, D.; Radusch, H. J. Polym Adv Technol 2003, 14, 19.
5. Pan, L.; Chiba, T.; Inoue, T. Polymer 2001, 42, 8825.
6. Araújo, J. R.; Vallim, M. R.; Spinacé, M. A. S.; De Paoli, M. A. J Appl Polym Sci 2008, 110, 1310.
7. Wang, H. G.; Jian, L. Q.; Pan, B. L.; Zhang, J. Y.; Yang, S. R.; Wang, H. G. Polym Eng Sci 2007, 47, 738.
8. Beltrame, P. L.; Castelli, A.; Pasquantonio, M. D.; Canetti, M.; Seves, A. J Appl Polym Sci 1996, 60, 579.
9. Yeh, J. T.; Huang, S. S.; Chen, H. Y. J Appl Polym Sci 2005, 97, 1333.
10. Yeh, J. T.; Huang, S. S.; Chen, H. Y. Polym Eng Sci 2005, 45, 25.
11. Yeh, J. T.; Jou, W. S.; Su, Y. S. J Appl Polym Sci 1999, 74, 2158.
12. Wei, Q.; Chionna, D.; Pracella, M. Macromol Chem Phys 2005, 206, 777.
13. Wei, Q.; Chionna, D.; Galoppini, E.; Pracella, M. Macromol Chem Phys 2003, 204, 1123.
14. Vocke, C.; Anttila, U.; Seppälä, J. J Appl Polym Sci 1999, 72, 1443.
15. La Mantia, F. P.; Scaffaro, R.; Valenza, A.; Marchetti, A.; Filippi, S. Macromol Symp 2003, 198, 173.
16. Filippi, S.; Chiono, V.; Polacco, G.; Paci, M.; Minkova, L. I.; Magagnini, P. Macromol Chem Phys 2002, 203, 1512.
17. Scaffaro, R.; La Mantia, F. P.; Canfora, L.; Polacco, G.; Filippi, S.; Magagnini, P. Polymer 2003, 44, 6951.
18. Yeh, J. T.; Jyan, C. F.; Yang, S. S.; Chou, S. Polym Eng Sci 1999, 39, 1952.
19. Baouz, T.; Fellahi, S. J Appl Polym Sci 2005, 98, 1748.
20. Krache, R.; Benachour, D.; Pötschke, P. J Appl Polym Sci 2004, 94, 1976.
21. Yao, Z. H.; Yin, Z. H.; Sun, G.; Liu, C. Z.; Tong, J.; Ren, L. Q.; Yin, J. H. J Appl Polym Sci 2000, 75, 232.
22. Kaito, A.; Iwakura, Y.; Li, Y.; Shimizu, H. J Macromol Sci Phys 2008, 47, 1062.
23. González-Nuñez, R.; Padilla, H.; De Kee, D.; Favis, B. D. Polym Bull 2001, 46, 323.
24. Boersma, A.; Turnhout, J. Polymer 1999, 40, 5023.
25. Coates, P. D.; Barnes, S. E.; Sibley, M. G.; Brown, E. C.; Edwards, H. G. M.; Scowen, I. J. Polymer 2003, 44, 5937.
26. Scherzer, T.; Müller, S.; Mehnert, R.; Volland, A.; Lucht, H. Polymer 2005, 46, 7072.
27. Wang, D.; Min, K. Polym Eng Sci 2005, 45, 998.
28. Kiehl, C.; Chu, L. L.; Letz, K.; Min, K. Polym Eng Sci 2001, 41, 1078.
29. Li, J.; Sun, Z.; Tatibouët, J.; Jen, C. K. Polym Eng Sci 2008, 48, 987.
30. Koulouri, E. G.; Gravalos, K. G.; Kallitsis, J. K. Polymer 1996, 37, 2555.
31. Ohlsson, B.; Hassander, H.; Törnell, B. Polymer 1998, 39, 6705.
32. Lin, C. M.; Wang, S.; Sun, H. M.; Li, J.; Guo, S. Y. Polym Eng Sci, to appear.
33. Wang, S.; Drda, P. A.; Inn, Y. W. J Rheol 1996, 40, 875.